Nonlinear Analysis: Modelling and Control, Vol. 22, No. 5, 579–597 ISSN 1392-5113
https://doi.org/10.15388/NA.2017.5.1

Ultimate boundary estimations and topological horseshoe analysis of a new 4D hyper-chaotic system*

Leilei Zhou[a], **Zengqiang Chen**[a,b], **Jiezhi Wang**[b], **Qing Zhang**[b]

[a]The Key Lab of Intelligent Robotics of Tianjin,
College of Computer and Control Engineering, Nankai University,
Tianjin 300353, China
chenzq@nankai.edu.cn

[b]College of Science, Civil Aviation University of China,
Tianjin 300300, China

Received: July 12, 2016 / **Revised:** May 22, 2017 / **Published online:** September 24, 2017

Abstract. In this paper, we first estimate the boundedness of a new proposed 4-dimensional (4D) hyper-chaotic system with complex dynamical behaviors. For this system, the ultimate bound set Ω_1 and globally exponentially attractive set Ω_2 are derived based on the optimization method, Lyapunov stability theory, and comparison principle. Numerical simulations are presented to show the effectiveness of the method and the boundary regions. Then, to prove the existence of hyper-chaos, the hyper-chaotic dynamics of the 4D nonlinear system is investigated by means of topological horseshoe theory and numerical computation. Based on the algorithm for finding horseshoes in three-dimensional hyper-chaotic maps, we finally find a horseshoe with two-directional expansions in the 4D hyper-chaotic system, which can rigorously prove the existence of the hyper-chaos in theory.

Keywords: hyper-chaotic system, ultimate bound, positively invariant set, globally exponentially attractive set, topological horseshoe.

1 Introduction

A 4D hyper-chaotic system is usually considered as a chaotic system with two positive Lyapunov exponents, which can enhance the randomness and unpredictability of the nonlinear system. So constructing a new hyper-chaotic system with complex dynamical behaviors may be more useful in some research fields, such as communication [1, 37], encryption [5, 20], and synchronization [3, 22, 31, 32].

It is well known that the dissipative chaotic system often has a typical strange attractor in its phase space and the strange attractor is usually bounded. Therefore, an interesting research topic is how to estimate the bound of the dissipative chaotic or hyper-chaotic

*This research was supported by Natural Science Foundation of China grant No. 61573199 and Tianjin Nature Science Foundation grant No. 14JCYBJC18700.

system. The ultimate bound is very important for the study of the qualitative behavior of a hyper-chaotic system. Besides, if one can prove that a hyper-chaotic system has a globally exponentially attractive set, one concludes that the system cannot have the equilibrium points, periodic or quasi-periodic solutions, or other chaotic or hyper-chaotic attractors existing outside the attractive set, which greatly simplifies the dynamics analysis of a chaotic or hyper-chaotic system. Furthermore, the boundedness of a chaotic system also plays an important role in chaos control and synchronization [21, 23, 24]. For example, in physical process control, if we use the high gain controller, it will result in the saturation of the actuator. The closed-loop performance of the system will be poor and even unstable. By estimating the ultimate boundary of the system attractive basin, a low gain controller can be designed to effectively deal with the problem of saturation constraint. Therefore, estimating the bound of attractive basin of chaotic system is helpful to the design of chaotic system control and synchronization scheme.

Although some researchers have investigated the ultimate bound property of the chaotic systems [17, 38], this is still a very difficult task technically for some high dimension systems. Ever since the Lorenz system was put forward, its ultimate bound has been investigated by Leonov et al. [6]. Li et al. [8] extended the results in the paper [7] and estimated the ultimate bounds for the Lorenz system family. Yu and Liao [36] estimated the ultimate bound and positively invariant set for a general chaotic system, which does not belong to the known Lorenz system or the Chen system, or the Lorenz family. Recently, by using the Lagrange multiplier method and set operations, Wang et al. [27] have estimated two kinds of explicit ultimate bound sets for a novel hyper-chaotic system. Therefore, it is meaningful to investigate the boundedness of the new proposed hyper-chaotic system based on the optimization method, Lyapunov stability theory, and comparison principle.

Besides, it is well known that, to prove the existence of hyper-chaos, the common method is calculating the Lyapunov exponents. However, numerical error is difficult to avoid [16], which makes this method not precise enough. The more reliable method is to verify the existence of hyper-chaos in theory. Topological horseshoe theory provides a more simple and convenient method to prove the existence of chaotic attractors, which is precisely effective. The method makes use of symbolic dynamics to study and describe the chaos from the invariant set. By combining the topological horseshoe theory with numerical simulations, it can not only give strict mathematical proof, but also reveal the dynamical mechanism [4, 19, 25].

The topological horseshoe theory has gradually shown its importance since Li and Yang [11] introduced it into the verification of hyper-chaotic system. Using the two-dimensional tensile horseshoe, the hyper-chaotic generation mechanisms of some classical systems have been strictly analyzed, and the existence of hyper-chaos has been also mathematically verified, such as MCK hyper-chaotic circuit [33], hyper-chaotic Henon mapping [12], Rössler hyper-chaotic system [9], the double coupling bridge oscillator system [13], and spacecraft power system [14], and so on. However, these achievements were only case researches and did not present a general algorithm. The reason is that it is too hard to find a topological horseshoe in a hyper-chaotic system due to the high dimension of the system and the multiple expansion directions in the state space. As we all know, a hyper-chaotic system usually has a large negative LE, its attractor is often

contracted closely to a certain surface. Based on this feature, we can use a remarkable algorithm proposed by Li and Tang [16] to detect a horseshoe with two-directional expansions effectively by deducting the dimension along the direction of contraction.

Motivated by the above discussions, a new 4D smooth quadratic autonomous hyper-chaotic system is constructed directly, and the complex dynamical behaviors are studied. We first investigate the boundedness of the new hyper-chaotic system. The ultimate bound and the positively invariant set Ω_1 are obtained, which is based on the optimization method and the comparison principle. Then we discuss the relationship between ultimate bound and the two positive Lyapunov exponents of the system. Besides, we find the globally exponentially attractive set Ω_2 of the system and conclude that the trajectories of the system go from the exterior of Ω_2 to the interior of Ω_2 at exponential rate. Here we use a combination of Lyapunov stability theory with the comparison principle method. Secondly, since the values of the two positive Lyapunov exponents are not large enough to tolerate the numerical errors during the computation, we give the computer-assisted verification of hyper-chaos. Based on the algorithm for finding horseshoes in three-dimensional hyper-chaotic maps, we find a horseshoe with two-directional expansions in the 4D hyper-chaotic system, which can rigorously prove the existence of the hyper-chaos in theory.

The organization of this paper is as follows. In Section 2, we will introduce mathematical model and study complex dynamical behaviors of the new proposed 4D hyper-chaotic system. In Section 3, we will estimate the boundedness of the new 4D hyper-chaotic system including the ultimate bound and the positively invariant set Ω_1 and the globally exponentially attractive set Ω_2. In Section 4, we will give the computer-assisted verification of hyper-chaos by virtue of the algorithm for finding horseshoes in three-dimensional hyper-chaotic maps. Finally, conclusions will be drawn in Section 5.

2 Mathematical model and complex dynamical behaviors

The new proposed 4D hyper-chaotic system is given as follows:

$$\begin{aligned} \dot{x} &= ay - ax + ezw, \\ \dot{y} &= bx - y - xz + w, \\ \dot{z} &= -cz + xy, \\ \dot{w} &= -ky - dw - gxz, \end{aligned} \tag{1}$$

where a, b, c, d, e, g, k are positive constant parameters determining the chaotic and hyper-chaotic behaviors of system (1).

2.1 Symmetry and invariant set

Since system (1) is invariant under the coordinate transformation $(x, y, z, w) \to (-x, -y, z, -w)$, it is symmetrical about z-axis.

z-axis is a positively invariant set of system (1), and we can get the equation $\dot{z} = -cz$ when the system is restricted to the z-axis. Since the solution of the equation is

$z(t) = z(t_0)\mathrm{e}^{-c(t-t_0)}$, the trajectories from arbitrary point on the z-axis will tend to $(0,0,0,0)$ when $t \to \infty$.

2.2 Dissipation

Denote $V(t)$ as the volume element and f as the vector field with components $(\dot{x}, \dot{y}, \dot{z}, \dot{w})$. According to the divergence theorem, we can get the following equation:

$$\frac{1}{V}\frac{\mathrm{d}V}{\mathrm{d}t} = \sum_{i=1}^{N}\frac{\partial f_i}{\partial x_i} = \nabla f = \frac{\partial \dot{x}}{\partial x} + \frac{\partial \dot{y}}{\partial y} + \frac{\partial \dot{z}}{\partial z} + \frac{\partial \dot{w}}{\partial w} = -(a + c + d + 1) < 0.$$

So system (1) is dissipative. That is to say, for the initial volume element $V(0)$, $V(t) = V(0)\mathrm{e}^{-(a+c+d+1)t}$ indicates that each volume element containing the trajectory of the system shrinks to zero at an exponential rate, and its dynamics behavior will be fixed on an attractor [28, 29]. Thus, system (1) is globally bounded.

2.3 The stability of equilibria

Before the detailed analysis, the study of equilibria is necessary. $S_0 = (0,0,0,0)$ is always a equilibrium point of system (1). Other equilibrium points can be shifted to S_0 by means of coordinate translation, so we just consider the stability of S_0. For the zero equilibrium point S_0, the characteristic equation is

$$\begin{aligned}\varphi(\lambda) = (\lambda + c)\big[&\lambda^3 + (a + d + 1)\lambda^2 + (a + d + k - ab + ad)\lambda \\ &+ ad + ak - abd\big] = 0.\end{aligned}$$

When $a = 18$, $b = 60$, $c = 8$, $d = 0.2$, $e = 0.1$, $g = 0.1$, $k = 10$, $a + d + k - ab + ad < 0$, the characteristic equation at least has one positive real eigenvalue. Therefore, the equilibrium point S_0 is unstable, which indicates that the system will generate chaos and hyper-chaos. The stability of the other equilibrium points of the system can be verified by the same method.

2.4 The rich dynamics evolution

The rich dynamics evolution of system (1) can be analyzed by Lyapunov exponents (LEs) spectrum, bifurcation diagram, and various phase portraits. Lyapunov exponents are the characteristic quantity obtained by the average of system's infinite long orbit and can be used to determine the existence and complexity of chaos and hyper-chaos. Now, the commonly used methods of calculating the LEs are QR decomposition method [2] and Wolf method [30]. In our paper, we use the QR decomposition method to calculate the LEs with the variation of parameter c. Bifurcation diagram is a intuitive representation of the system evolutionary process. The key to drawing bifurcation diagram is to find a suitable Poincaré section. The horizontal axis of bifurcation diagram is the system parameter, while the vertical axis is the value of a state variable. In our paper, we give the bifurcation diagram versus parameter c.

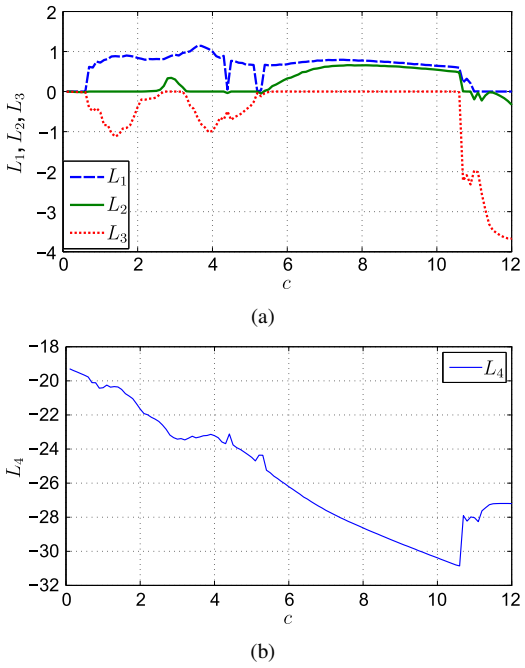

Figure 1. The Lyapunov exponents spectrum versus $c \in [0, 12]$ with $a = 18$, $b = 60$, $d = 0.2$, $e = 0.1$, $g = 0.1$, $k = 10$.

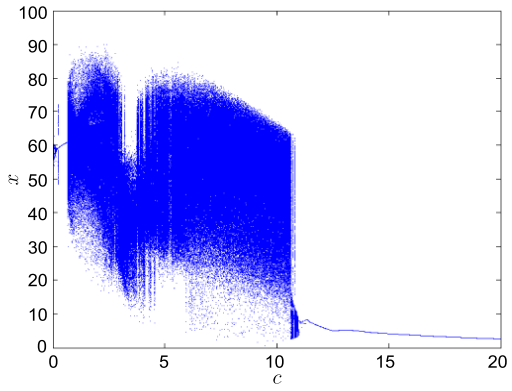

Figure 2. The bifurcation diagram versus $c \in [0, 20]$ with $a = 18$, $b = 60$, $d = 0.2$, $e = 0.1$, $g = 0.1$, $k = 10$.

Let $a = 18$, $b = 60$, $d = 0.2$, $e = 0.1$, $g = 0.1$, $k = 10$, and the parameter c varies. Denote the four LEs of system (1) by L_1, L_2, L_3, L_4, which satisfy $L_1 > L_2 > L_3 > L_4$. The LEs spectrum and the corresponding bifurcation diagram versus c are shown in Figs. 1 and 2, respectively. With the variation of parameter c, system (1) undergoes periodic, quasi-periodic, chaotic, and hyper-chaotic state. The typical attractors are shown

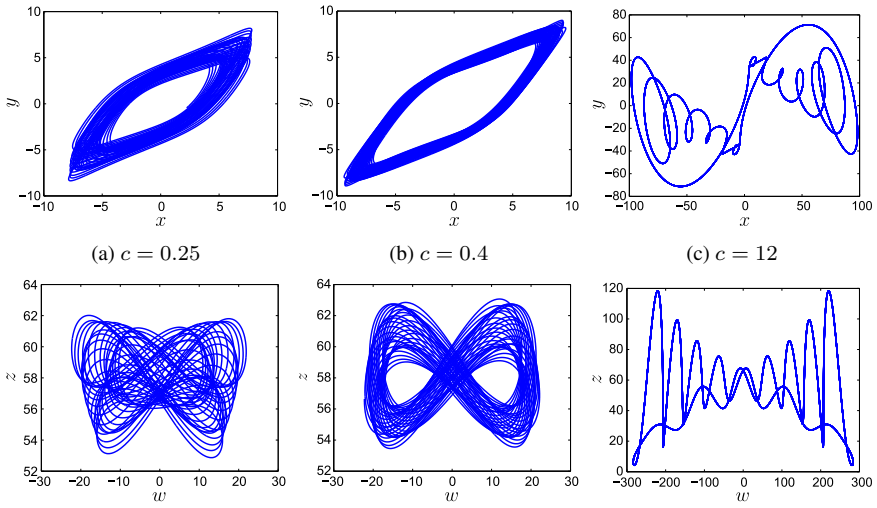

(a) $c = 0.25$ (b) $c = 0.4$ (c) $c = 12$

(d) $c = 0.25$ (e) $c = 0.4$ (f) $c = 12$

Figure 3. Phase portraits of quasi-periodic and periodic attractors of system (1) versus c with $a = 18$, $b = 60$, $d = 0.2$, $e = 0.1$, $g = 0.1$, $k = 10$.

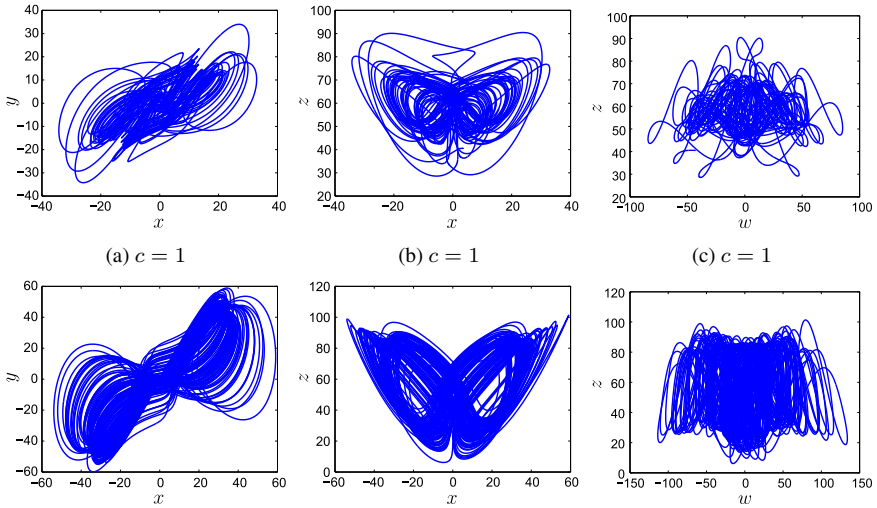

(a) $c = 1$ (b) $c = 1$ (c) $c = 1$

(d) $c = 8$ (e) $c = 8$ (f) $c = 8$

Figure 4. Phase portraits of chaotic and hyper-chaotic attractors of system (1) versus c with $a = 18$, $b = 60$, $d = 0.2$, $e = 0.1$, $g = 0.1$, $k = 10$.

in Figs. 3 and 4. Figure 3 shows phase portraits of quasi-periodic and periodic attractors of system (1). Figure 4 shows phase portraits of chaotic and hyper-chaotic attractors of system (1). Especially, the system is in hyper-chaotic state when $c = 8$, the four LEs are $L_1 = 0.7742$, $L_2 = 0.6539$, $L_3 = -0.0001$, $L_4 = -28.6280$.

3 Boundedness of the new hyper-chaotic system

3.1 Preliminary

In this subsection, we will introduce some basic definitions, which are necessary for proving the proposed theorems in the following two subsections.

Consider the following autonomous system:

$$\dot{X} = f(X), \tag{2}$$

where $X = (x_1, x_2, \ldots, x_n)^{\mathrm{T}} \in \mathbb{R}^n$, $f : \mathbb{R}^n \to \mathbb{R}^n$, $t_0 > 0$ is the initial time, $X(t, t_0, X_0)$ is the solution, which satisfies $X(t_0, t_0, X_0) = X_0$. Suppose $\Omega \subset \mathbb{R}^n$ is a compact set, and the distance between $X(t, t_0, X_0)$ and Ω is defined by

$$\rho\big(X(t, t_0, X_0), \Omega\big) = \inf_{\hat{X} \in \Omega} \big\|X\big(t, t_0, X_0\big) - \hat{X}\big\|.$$

Denote $\Omega_\varepsilon = \{X \mid \rho(X, \Omega) < \varepsilon\}$. Thus, one gets $\Omega \subset \Omega_\varepsilon$.

Definition 1. (See [26].) Suppose $\Omega \subset \mathbb{R}^n$ is a compact set satisfying

$$\lim_{t \to \infty} \rho\big(X(t), \Omega\big) = 0$$

for all $X_0 \in \mathbb{R}^n \setminus \Omega$, that is, for any $\varepsilon > 0$, there exists $T > t_0$ satisfying $X(t, t_0, X_0) \in \Omega_\varepsilon$ for all $t \geqslant T$. Then the set Ω is called an ultimate bound of system (2). If for any $X_0 \in \Omega$ and all $t \geqslant t_0$, $X(t, t_0, X_0) \in \Omega$, then Ω is called the positively invariant set for system (2).

Definition 2. (See [18].) For autonomous system (2), if there exist generalized positive definite and radially unbounded Lyapunov function $V(X(t))$ and constants $L > 0$, $\beta > 0$, for all $X_0 \in \mathbb{R}^n$, when $V(X(t)) > L$, $V(X_0) > L$, $t > t_0$, the following inequality is satisfied:

$$V\big(X(t)\big) - L \leqslant \big[V(X_0) - L\big]\mathrm{e}^{-\beta(t-t_0)},$$

then

$$\Omega = \Big\{X \;\Big|\; \overline{\lim}_{t \to +\infty} V\big(X(t)\big) \leqslant L\Big\}$$

is said to be a globally exponentially attractive set of system (2).

3.2 The ultimate bound and positively invariant set

In this subsection, we will estimate the ultimate bound and positively invariant set of the system for $a > 0$, $b > 0$, $c > 0$, $d > 0$, $e > 0$, $g > 0$, $k > 0$. Before the detailed study, let us introduce the following lemma.

Lemma 1. *Define a set* $\Gamma = \{(x,y,z,w) \mid x^2/\tilde{a}^2 + y^2/\tilde{b}^2 + (z-\tilde{c})^2/\tilde{c}^2 + w^2/\tilde{d}^2 = 1, \tilde{a} \neq 0, \tilde{b} \neq 0, \tilde{c} \neq 0, \tilde{d} \neq 0\}$ *and* $G(x,y,z,w) = x^2+y^2+z^2+w^2$, $H(x,y,z,w) = x^2+y^2+(z-2\tilde{c})^2+w^2$, $(x,y,z,w) \in \Gamma$. *Then we can get*

$$G_m = \max_{(x,y,z,w)\in\Gamma} G = H_m = \max_{(x,y,z,w)\in\Gamma} H = \begin{cases} \frac{\tilde{a}^4}{\tilde{a}^2-\tilde{c}^2}, & \tilde{a} \geqslant \tilde{b},\ \tilde{a} \geqslant \tilde{d},\ \tilde{a} \geqslant \sqrt{2}\tilde{c}, \\ \frac{\tilde{b}^4}{\tilde{b}^2-\tilde{c}^2}, & \tilde{b} > \tilde{a},\ \tilde{b} \geqslant \tilde{d},\ \tilde{b} \geqslant \sqrt{2}\tilde{c}, \\ \frac{\tilde{d}^4}{\tilde{d}^2-\tilde{c}^2}, & \tilde{d} > \tilde{a},\ \tilde{d} > \tilde{b},\ \tilde{d} \geqslant \sqrt{2}\tilde{c}, \\ 4\tilde{c}^2, & \tilde{a} < \sqrt{2}\tilde{c},\ \tilde{b} < \sqrt{2}\tilde{c},\ \tilde{d} < \sqrt{2}\tilde{c}. \end{cases}$$

Proof. It can be easily proved by the Lagrange multiplier method. □

By Lemma 1, we can get the following theorem.

Theorem 1. *For* $a > 0$, $b > 0$, $c > 0$, $d > 0$, $e > 0$, $g > 0$, $k > 0$, $h > 0$, *the following set is the ultimate bound and positively invariant set of the system*:

$$\Omega_1 = \left\{ (x,y,z,w) \;\middle|\; x^2 + hy^2 + h\left(z - \frac{a+hb}{h}\right)^2 + \frac{e}{g}w^2 \leqslant R^2 \right\}. \tag{3}$$

Here

$$R^2 = \begin{cases} \frac{(a+hb)^2c^2}{4ha(c-a)}, & a \leqslant 1,\ a \leqslant d,\ c \geqslant 2a, \\ \frac{(a+hb)^2c^2}{4h(c-1)}, & a > 1,\ d \geqslant 1,\ c \geqslant 2, \\ \frac{(a+hb)^2c^2}{4hd(c-d)}, & a > d,\ d < 1,\ c \geqslant 2d, \\ \frac{(a+hb)^2}{h}, & c < 2a,\ c < 2,\ c < 2d. \end{cases}$$

Proof. Define the following generalized positive definite and radially unbounded Lyapunov function:

$$V_1 = x^2 + hy^2 + h\left(z - \frac{a+hb}{h}\right)^2 + \frac{e}{g}w^2, \tag{4}$$

where $h = ke/g > 0$. Computing the derivative of V_1 along the trajectory of system (1), we can obtain

$$\begin{aligned} \frac{\mathrm{d}V_1}{\mathrm{d}t} &= 2x\dot{x} + 2hy\dot{y} + 2h\left(z - \frac{a+hb}{h}\right)\dot{z} + 2\frac{e}{g}w\dot{w} \\ &= 2x(ay - ax + ezw) + 2hy(bx - y - xz + w) \\ &\quad + 2h\left(z - \frac{a+hb}{h}\right)(-cz + xy) + 2\frac{e}{g}w(-ky - dw - gxz) \end{aligned}$$

$$= -2ax^2 - 2hy^2 - 2hcz^2 + 2(a+hb)cz - 2\frac{de}{g}w^2$$
$$= -2ax^2 - 2hy^2 - 2hc\left[z - \frac{(a+hb)}{2h}\right]^2 - 2\frac{de}{g}w^2 + \frac{(a+hb)^2c}{2h}.$$

Obviously, V_1 is positive definite for $a > 0$, $b > 0$, $c > 0$, $d > 0$, $e > 0$, $g > 0$, $k > 0$, $h > 0$. Let $\dot{V}_1 = 0$, then the following ellipsoidal surface Γ can be obtained:

$$2ax^2 + 2hy^2 + 2hc\left[z - \frac{(a+hb)}{2h}\right]^2 + 2\frac{de}{g}w^2 = \frac{(a+hb)^2c}{2h}. \tag{5}$$

Outside Γ, $\dot{V}_1 < 0$, while inside Γ, $\dot{V}_1 > 0$. Thus, the ultimate bound of system (1) can be only reached on Γ. Since the $V_1(X)$ is a continuous function and Γ is a bounded close set, function (4) can reach its maximum value: $\max V_1(X)_{X\in\Gamma} = R^2$ on the surface Γ defined in Eq. (5). Obviously, the set defined by $\{(x,y,z,w) \mid V_1(X) \leqslant \max V_1(X), (x,y,z,w) \in \Gamma\}$ contains the solutions of system (1). By solving the following conditional extremum problem, we can get the maximum value $\max V_1(X)$:

$$\begin{aligned} &\max V_1 = \max\left\{x^2 + hy^2 + h\left(z - \frac{a+hb}{h}\right)^2 + \frac{e}{g}w^2\right\}, \\ &\text{s.t. } \frac{x^2}{\frac{(a+hb)^2c}{4ha}} + \frac{hy^2}{\frac{(a+hb)^2c}{4h}} + \frac{h(z-\frac{a+hb}{2h})^2}{\frac{(a+hb)^2}{4h}} + \frac{\frac{e}{g}w^2}{\frac{(a+hb)^2c}{4hd}} = 1. \end{aligned} \tag{6}$$

Set $x = \tilde{x}$, $\sqrt{h}y = \tilde{y}$, $\sqrt{h}z = \tilde{z}$, $\sqrt{e/g}\,w = \tilde{w}$ as a new variable, and denote $(a+hb)^2c/(4ha) = \tilde{a}^2$, $(a+hb)^2c/(4h) = \tilde{b}^2$, $(a+hb)^2/(4h) = \tilde{c}^2$, $(a+hb)^2c/(4hd) = \tilde{d}^2$, then the conditional extremum problem (6) can be transformed into the following forms:

$$\begin{aligned} &\max V_1 = \max\left\{\tilde{x}^2 + \tilde{y}^2 + (\tilde{z} - 2\tilde{c})^2 + \tilde{w}^2\right\}, \\ &\text{s.t. } \frac{\tilde{x}^2}{\tilde{a}^2} + \frac{\tilde{y}^2}{\tilde{b}^2} + \frac{(\tilde{z}-\tilde{c})^2}{\tilde{c}^2} + \frac{\tilde{w}^2}{\tilde{d}^2} = 1. \end{aligned} \tag{7}$$

According to Lemma 1, we can easily get

$$\max_{(x,y,z,w)\in\Gamma} V_1(X) = R^2 = \begin{cases} \frac{(a+hb)^2c^2}{4ha(c-a)}, & a \leqslant 1,\ a \leqslant d,\ c \geqslant 2a, \\ \frac{(a+hb)^2c^2}{4h(c-1)}, & a > 1,\ d \geqslant 1,\ c \geqslant 2, \\ \frac{(a+hb)^2c^2}{4hd(c-d)}, & a > d,\ d < 1,\ c \geqslant 2d, \\ \frac{(a+hb)^2}{h}, & c < 2a,\ c < 2,\ c < 2d. \end{cases}$$

Therefore, we have obtained the compact set Ω_1 given in Eq. (3). According to Definition 1, since $\Gamma \subset \Omega_1$, next we will use the reduction to absurdity to prove

$$\lim_{t\to+\infty} \rho\big(X(t), \Omega_1\big) = 0. \tag{8}$$

Here $X(t) = (x(t), y(t), z(t), w(t))$. Suppose Eq. (8) does not hold, we can conclude that the orbits of system (1) are outside Ω_1, thus $\dot{V}_1 < 0$ and $V_1(X(t))$ monotonously decreases.

Let $\lim_{t\to+\infty} V_1(X(t)) = \tilde{V}_1 > R^2$, and $\delta = \inf_{X\in D}(-\dot{V}_1(X(t)))$, where $D = \{X(t) \mid \tilde{V}_1 \leqslant V_1(X(t)) \leqslant V_1(X(t_0))\}$, t_0 is the initial time. Consequently, we have that δ, $\tilde{V}_1$ are both positive constants and $\mathrm{d}V_1(X(t))/\mathrm{d}t \leqslant -\delta$. As $t \to +\infty$, we can obtain

$$0 < V_1\big(X(t)\big) \leqslant V_1\big(X(t_0)\big) - \delta(t - t_0) \to -\infty.$$

This is inconsistent, thus Eq. (8) holds, it is equivalent to say that the set Ω_1 is the ultimate bound set of system (1).

Then we prove that Ω_1 is also the positively invariant set of system (1). Suppose $V_1(X(t))$ attains its maximum value on surface Γ at the point $P_0(\tilde{x_0}, \tilde{y_0}, \tilde{z_0}, \tilde{w_0})$. Since Γ is contained in Ω_1, for any point $X(t)$ on Γ and $X(t) \neq P_0$, we have $\dot{V}_1 < 0$. Thus, any orbit $X(t)$ ($X(t) \neq P_0$) of system (1) will go into the set Ω_1. When $X(t) = P_0$, by the continuation theorem, $X(t)$ will also go into the set Ω_1. Summarizing the contents above, we conclude that Ω_1 is positively invariant set of system (1). This completes the proof. □

Numerical simulations

(i) When $a = 18$, $b = 60$, $c = 8$, $d = 0.2$, $e = 0.1$, $g = 0.1$, $k = 10$, the system is in hyper-chaotic state, the four LEs: $L_1 = 0.7742$, $L_2 = 0.6539$, $L_3 = -0.0001$, $L_4 = -28.6280$. The ultimate bound and positively invariant set Ω_1 is

$$\Omega_1 = \big\{(x, y, z, w) \;\big|\; x^2 + 10y^2 + 10(z - 61.8)^2 + w^2 \leqslant 391716.923\big\}.$$

(ii) When $a = 16$, $b = 46$, $c = 6$, $d = 0.2$, $e = 0.1$, $g = 0.1$, $k = 8$, the system is in hyper-chaotic state, the four LEs: $L_1 = 0.5707$, $L_2 = 0.5029$, $L_3 = -0.0006$, $L_4 = -24.2731$. The ultimate bound and positively invariant set Ω_1 is

$$\Omega_1 = \big\{(x, y, z, w) \;\big|\; x^2 + 8y^2 + 8(z - 48)^2 + w^2 \leqslant 143006.897\big\}.$$

(iii) When $a = 10$, $b = 30$, $c = 3$, $d = 0.1$, $e = 0.08$, $g = 0.06$, $k = 3.8$, the system is in hyper-chaotic state, the four LEs: $L_1 = 0.3906$, $L_2 = 0.3546$, $L_3 = -0.0003$, $L_4 = -14.8448$. The ultimate bound and positively invariant set Ω_1 is

$$\Omega_1 = \big\{(x, y, z, w) \;\big|\; x^2 + 5.07y^2 + 5.07(z - 31.97)^2 + 1.33w^2 \leqslant 40210.7886\big\}.$$

In Figs. 5–7, we give the phase portraits and ultimate bound of system (1) in 3D and 2D planes with corresponding parameter values. By comparison, we can find that with the variation of parameter values, the two positive LEs becomes smaller, and the corresponding Ω_1 also becomes smaller.

Although Theorem 1 gives the ultimate bound and positively invariant set of system (1), it does not give the estimation of the trajectories rate. In Section 3.3, we will give the globally exponentially attractive set to estimate the trajectories rate.

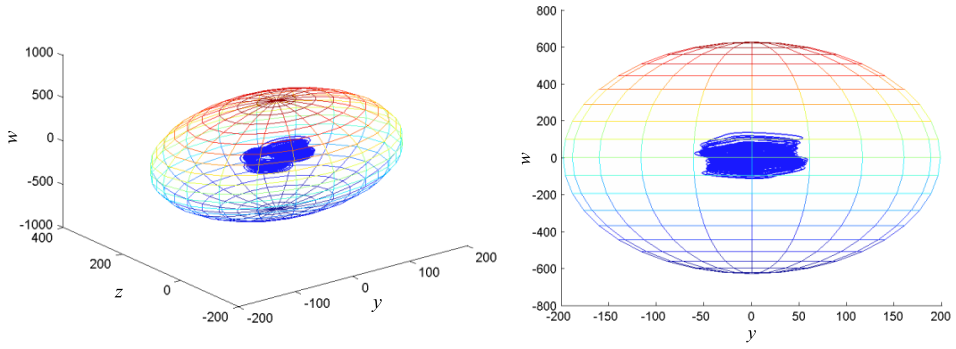

(a) (b)

Figure 5. The phase portraits and ultimate bound of system (1) with $a = 18$, $b = 60$, $c = 8$, $d = 0.2$, $e = 0.1$, $g = 0.1$, $k = 10$.

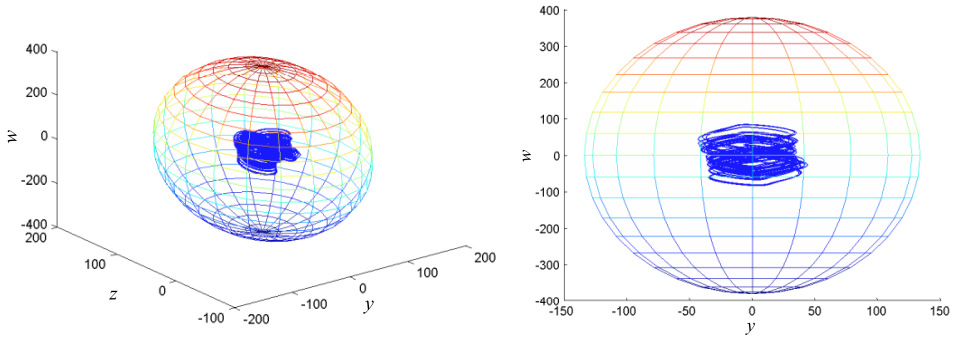

(a) (b)

Figure 6. The phase portraits and ultimate bound of system (1) with $a = 16$, $b = 46$, $c = 6$, $d = 0.2$, $e = 0.1$, $g = 0.1$, $k = 8$.

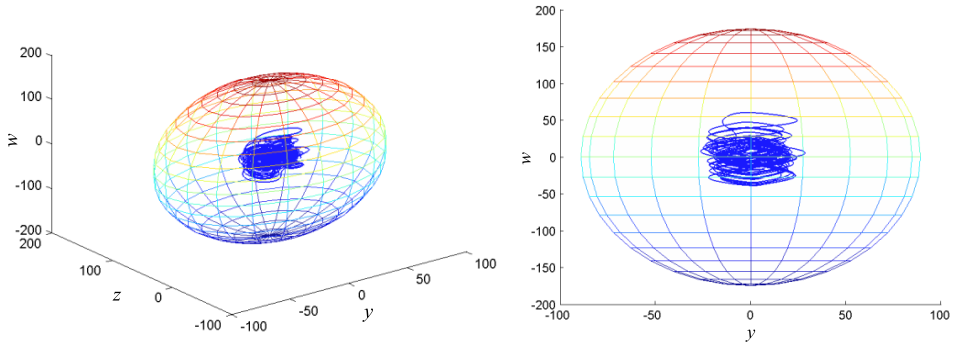

(a) (b)

Figure 7. The phase portraits and ultimate bound of system (1) with $a = 10$, $b = 30$, $c = 3$, $d = 0.1$, $e = 0.08$, $g = 0.06$, $k = 3.8$.

3.3 The globally exponentially attractive set

The objective of this subsection is to derive the globally exponentially attractive set of the hyper-chaotic system (1).

Theorem 2. *For all $a > 0$, $b > 0$, $c > 0$, $d > 0$, $k > 0$, $e > 0$, $g > 0$, and $h > 0$, let*

$$V\big(X(t)\big) = x^2 + hy^2 + h\bigg(z - \frac{a+hb}{h}\bigg)^2 + \frac{e}{g}w^2,$$

$$X(t) = \big(x(t), y(t), z(t), w(t)\big),$$

$$\beta = \min\{a, c, d, 1\}, \qquad L = \frac{(a+hb)^2 c}{\beta h}.$$

When $V(X(t)) > L$, $V(X_0) > L$, $t \geqslant t_0$, we can get an exponential estimation of system (1) *given by*

$$V\big(X(t)\big) - L \leqslant \big[V(X_0) - L\big]\mathrm{e}^{-\beta(t-t_0)}.$$

Especially, the set

$$\Omega_2 = \bigg\{X \;\bigg|\; x^2 + hy^2 + h\bigg(z - \frac{a+hb}{h}\bigg)^2 + \frac{e}{g}w^2 \leqslant L\bigg\}$$

is a globally exponentially attractive set of system (1).

Proof. Define the following generalized positive definite and radially unbounded Lyapunov function:

$$V\big(X(t)\big) = x^2 + hy^2 + h\bigg(z - \frac{a+hb}{h}\bigg)^2 + \frac{e}{g}w^2.$$

Here $h = ke/g > 0$.

Computing the derivative of $V(X(t))$ along the trajectory of system (1) when $V(X(t)) > L$, $V(X_0) > L$, $t \geqslant t_0$, we have

$$\begin{aligned}
\frac{\mathrm{d}V(X(t))}{\mathrm{d}t} &= 2x\dot{x} + 2hy\dot{y} + 2h\bigg(z - \frac{a+hb}{h}\bigg)\dot{z} + \frac{2e}{g}w\dot{w} \\
&= 2x(ay - ax + ezw) + 2hy(bx - y - xz + w) \\
&\quad + 2h\bigg(z - \frac{a+hb}{h}\bigg)(-cz + xy) + \frac{2e}{g}w(-ky - dw - gxz) \\
&= -2ax^2 - 2hy^2 - 2hcz^2 + 2(a+hb)cz - \frac{2de}{g}w^2 \\
&= -ax^2 - hy^2 - hc\bigg(z - \frac{a+hb}{h}\bigg)^2 - \frac{de}{g}w^2 \\
&\quad + \frac{(a+hb)^2 c}{h} - ax^2 - hy^2 - hcz^2 - \frac{de}{g}w^2
\end{aligned}$$

$$\begin{aligned}
&\leqslant -\beta\left[x^2 + hy^2 + h\left(z - \frac{a+hb}{h}\right)^2 + \frac{e}{g}w^2\right] + \frac{(a+hb)^2 c}{h} \\
&= -\beta V(X(t)) + \frac{(a+hb)^2 c}{h} = -\beta\left[V\big(X(t)\big) - \frac{(a+hb)^2 c}{\beta h}\right] \\
&= -\beta\big[V\big(X(t)\big) - L\big] < 0.
\end{aligned}$$

This is equivalent to say

$$\frac{\mathrm{d}V(X(t))}{\mathrm{d}t} \leqslant -\beta\big[V\big(X(t)\big) - L\big]. \tag{9}$$

By the comparison theorem and integrating both sides of formula (9) we obtain

$$\begin{aligned}
V\big(X(t)\big) &\leqslant V\big(X(t_0)\big)\mathrm{e}^{-\beta(t-t_0)} + \int_{t_0}^{t} \beta L \mathrm{e}^{-\beta(t-\tau)}\,\mathrm{d}\tau \\
&= V\big(X(t_0)\big)\mathrm{e}^{-\beta(t-t_0)} + L\big(1 - \mathrm{e}^{-\beta(t-t_0)}\big).
\end{aligned}$$

Thus, if $V(X(t)) > L, V(X_0) > L, t \geqslant t_0$, we have the following exponential estimation for system (1):

$$V\big(X(t)\big) - L \leqslant \big[V\big(X(t_0)\big) - L\big]\mathrm{e}^{-\beta(t-t_0)}.$$

By the definition, taking limit on both sides of the above inequality as $t \to +\infty$, we can get

$$\overline{\lim_{t\to+\infty}} V\big(X(t)\big) \leqslant L.$$

Namely, the set

$$\Omega_2 = \left\{(x,y,z,w) \;\middle|\; x^2 + hy^2 + h\left(z - \frac{a+hb}{h}\right)^2 + \frac{e}{g}w^2 \leqslant L\right\}$$

is the globally exponentially attractive set of system (1). This completes the proof. □

Numerical simulations

(i) When $a = 16$, $b = 46$, $c = 6$, $d = 0.8$, $e = 0.1$, $g = 0.1$, $k = 8$, the system is in hyper-chaotic state, the four LEs: $L_1 = 0.4093$, $L_2 = 0.2332$, $L_3 = -0.0002$, $L_4 = -24.4424$. The globally exponentially attractive set Ω_2 is

$$\Omega_2 = \big\{(x,y,z,w) \;\big|\; x^2 + 8y^2 + 8(z-48)^2 + w^2 \leqslant 138240\big\}.$$

(ii) When $a = 16$, $b = 46$, $c = 6$, $d = 0.8$, $e = 0.1$, $g = 0.1$, $k = 1$, the system is in chaotic state, the four LEs: $L_1 = 1.3422$, $L_2 = 0$, $L_3 = -1.0335$, $L_4 = -24.1086$. The globally exponentially attractive set Ω_2 is

$$\Omega_2 = \big\{(x,y,z,w) \;\big|\; x^2 + y^2 + (z-62)^2 + w^2 \leqslant 28830\big\}.$$

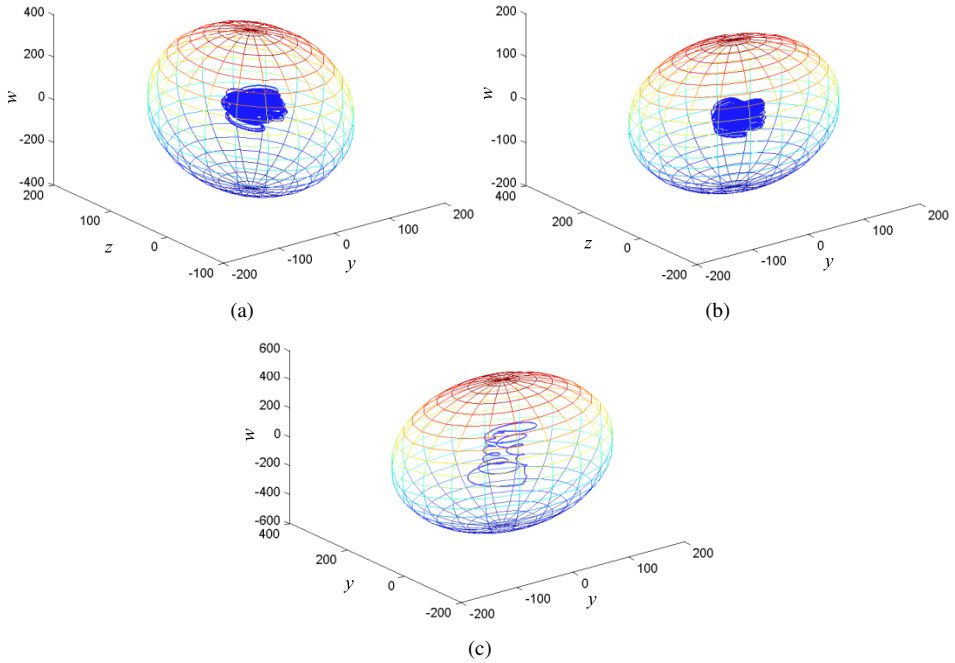

Figure 8. The trajectories of system (1) are contained in Ω_2 with $a = 16$, $b = 46$, $c = 6$, $d = 0.8$, $e = 0.1$, $g = 0.1$, $k = 8$.

(iii) When $a = 16$, $b = 46$, $c = 11$, $d = 0.8$, $e = 0.1$, $g = 0.1$, $k = 8$, the system is in periodic state, the four LEs: $L_1 = 0.0003$, $L_2 = -0.1727$, $L_3 = -2.8119$, $L_4 = -25.8157$. The globally exponentially attractive set Ω_2 is

$$\Omega_2 = \left\{(x, y, z, w) \;\middle|\; x^2 + 8y^2 + 8(z - 62)^2 + w^2 \leqslant 253440\right\}.$$

Through the analysis of the above conditions, we can find that the trajectories of system (1) go from the exterior of Ω_2 to the interior of Ω_2 at exponential rate and when $t \to +\infty$, the trajectories of system (1) are contained in Ω_2 as shown in Fig. 8. That is to say, the system cannot have the equilibrium points, periodic or quasi-periodic solutions, or other chaotic or hyper-chaotic attractors existing outside the attractive set.

4 Computer-assisted verification of hyper-chaos

From the analysis in Sections 2 and 3 we can find that system (1) is hyper-chaotic for different parameters. One important difference among them is the values of two positive Lyapunov exponents. In Section 3, when parameters $a = 10$, $b = 30$, $c = 3$, $d = 0.1$, $e = 0.08$, $g = 0.06$, $k = 3.8$, the two positive Lyapunov exponents are $L_1 = 0.3906$,

$L_2 = 0.3546$, respectively. The two positive Lyapunov exponents may be not large enough to tolerate the numerical errors during the computation. So it is significant to find a more reliable method to prove the existence of hyper-chaos. In our cases, we will introduce a rigourous proof of the existence of hyper-chaos in system (1) by directly detecting topological horseshoes with two-directional expansions in the corresponding Poincaré map.

Before the detailed study, some theoretical criteria of topological horseshoes are firstly reviewed, and then we will present our main results.

Let X be a metric space, and D is a compact subset of X. There are m completely disjoint connected compact subsets $D_1, D_2, \ldots, D_m$ of D. For each D_i, $1 \leqslant i \leqslant m$, let D_i^1 and D_i^2 be its two mutually disjoint connected nonempty compact subsets contained in the boundary of ∂D_i. Let the map f be continuous on each D_i.

Definition 3. (See [9].) Let $\Gamma \subset D_i$ be a connected subset. Γ is said to be a separation of D_i^1 and D_i^2, denoted by $\Gamma \updownarrow (D_i^1, D_i^2)$, if for any connected subset $L \subset D_i$ with $L \cap D_i^1 = \emptyset$ and $L \cap D_i^2 = \emptyset$, one has $\Gamma \cap L \neq \emptyset$.

Definition 4. (See [9,34].) Let $\Gamma \subset D_i$ be a compact subset. We say that $f(\Gamma)$ separates D_j with respect to D_j^1 and D_j^2 if Γ contains a compact subset Γ' such that $f(\Gamma') \updownarrow (D_j^1, D_j^2)$, we denote it by $f(\Gamma) \mapsto D_j$. If $f(\Gamma) \mapsto D_j$ holds true for each subset $\Gamma \subset D_i$ satisfied $\Gamma \updownarrow (D_i^1, D_i^2)$, we say that $f : D_i \mapsto D_j$ is a codimension-one crossing with respect to two pairs (D_i^1, D_i^2) and (D_j^1, D_j^2).

Theorem 3. (*See* [34].) *If the codimension-one crossing relation $f : D_i \mapsto D_j$, holds for $1 \leqslant i, j \leqslant m$, then there exists a compact invariant set $K \subset D$ such that $f|K$ is semi-conjugate to the m-shift mapping. Then the entropy of f satisfies* $\operatorname{ent}(f) \geqslant \log m$.

Sometimes for verifying existence of chaos, the assumption in Theorem 3 is not easy to be satisfied in practice. So we use the following practical corollary.

Corollary 1. (*See* [9].) *Suppose that the map $f : D \to X$ satisfies the following assumptions*:

(i) *There exist two mutually disjoint compact subsets D_1 and D_2 of D, and $f^m|D_1$ and $f^n|D_2$ are homeomorphisms, where m, n are positive integers.*

(ii) *$f^m(D_1) \mapsto D_1$, $f^m(D_1) \mapsto D_2$, $f^n(D_2) \mapsto D_1$, and $f^n(D_2) \mapsto D_2$.*

Then there exists a compact invariant set $K \subset D$, such that $f^{m+n}|K$ is semiconjugate to 2-shift dynamics, and the topological entropy of f satisfies $\operatorname{ent}(f) \geqslant \log 2/(m+n)$.

Since f in the above corollary is a homeomorphism, we are going to study a Poincaré map of system (1). By taking the hyperplane $\Pi = \{\mathbf{x} \stackrel{\Delta}{=} (x, y, z, w) \mid x = 0, \dot{x} > 0\}$ as a Poincaré cross-section, the corresponding Poincaré map $P : \Pi \to \Pi$ can be defined as follows: for each $\mathbf{x} = (0, y, z, w) \in \Pi$, $P(\mathbf{x})$ is taken to be the first return point in Π under the flow of the dynamical system with the initial condition $\mathbf{x}$.

Different from many other studies on topological horseshoes for two-dimensional (2D) chaotic maps [10, 15, 35], it is too hard to find a horseshoe directly for three-dimensional (3D) chaotic maps due to the higher dimensionality. Hence, we utilize the

following technique to make it possible. Firstly, we deduct the dimension along the direction of contraction to get a 2D projective map. Then we detect a projective horseshoe with two-directional expansion. At last, we construct a 3D horseshoe back to the original map P. According to the algorithm, we find a horseshoe by three steps.

(i) Due to the large negative LE, the dynamics in this direction contract very quickly, and the hyper-chaotic attractor is often contracted closely to a curved surface whose equation $w = s(y, z)$ can be easily fitted in MATLAB. Hence, we deduct the dimension along the direction of contraction to obtain a 2D projective system.

(ii) Now, we only need to cast about for a 2D horseshoe of the projective map on the yoz-plane. Through several attempts, we find a horseshoe with two directional expansions by choosing two quadrilaterals in the yoz-plane. The four vertices of the first quadrilateral A_{yoz} in terms of (y, z) are $A_1 = (23.107, 0.522)$, $A_2 = (21.321, 0.125)$, $A_3 = (25.607, -1.125)$, $A_4 = (26.964, -0.639)$. The four vertices of the second one B_{yoz} are $B_1 = (20.178, -0.123)$, $B_2 = (18.821, -0.282)$, $B_3 = (21.107, -1.165)$, $B_4 = (22.428, -1.075)$.

(iii) We construct the 3D horseshoe of the map P utilizing the projective horseshoe by projecting the planar horseshoe back to the 3D space. Finally, we have two blocks A and B in the phase space of the Poincaré map P as shown in Figs. 9(a) and 10(a). It is not hard to get the following theorem.

Theorem 4. *For the Poincaré map $P : \Pi \to \Pi$, there exists a closed invariant set $\Lambda \subset A \bigcup B$ on which $P^{1+2}|\Lambda$ is semi-conjugate to the 2-shift, and* $\mathrm{ent}(P) \geqslant \log 2/3$.

Proof. According to Corollary 1, we only need to show that A, B, and their images under P and P^2 respectively satisfy the following relationships about the codimension-one crossing:

$$P(A) \mapsto A, \qquad P(A) \mapsto B, \qquad P^2(B) \mapsto A, \qquad P^2(B) \mapsto B.$$

The geometrical relations of A, B and $P(A)$ are shown in Fig. 9. Figure 9(a) is a 3D view, which suggests that $P(A)$ expands in two directions and transversely intersects both blocks A and B. Figure 9(b) is a side view, which shows that the intersection happens between their top and bottom surfaces, i.e., (A^t, A^b) and (B^t, B^b). Figure 9(c) is a top view, which shows that the side surface of A is mapped outside A and B. Therefore, for each separation S of (A^t, A^b), $f(S) \bigcap A$ must be a separation of (A^t, A^b), and $f(S) \bigcap B$ must be a separation of (B^t, B^b). Then we have $P(A) \mapsto A, P(A) \mapsto B$. Similarly, we can have $P^2(B) \mapsto A, P^2(B) \mapsto B$ from the Fig. 10.

Since system (1) is smooth, i.e., the system has a unique solution from each initial condition, Figs. 9 and 10 also show that $P|A$ and $P^2|B$ are both continuous, so they must be homeomorphism. Then it follows from Corollary 1 that there exists a compact invariant set $\Lambda \subset A \bigcup B$ such that $P^{1+2}|\Lambda$ is semi-conjugate to the 2-shift, and the topological entropy of P is not less than $\log 2/3$. Since $P|A$ and $P^2|B$ both expand in two directions, the expansions along each trajectory in Λ are also in two directions, so there must exist two positive Lyapunov exponents. Therefore, system (1) is hyper-chaotic. □

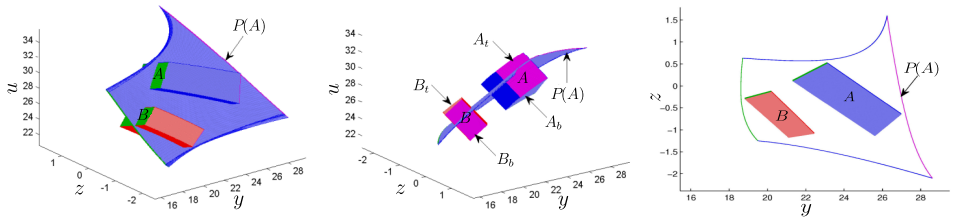

(a) 3D view (b) Side view (c) Top view

Figure 9. $P(A)$ separates A and B under system (1).

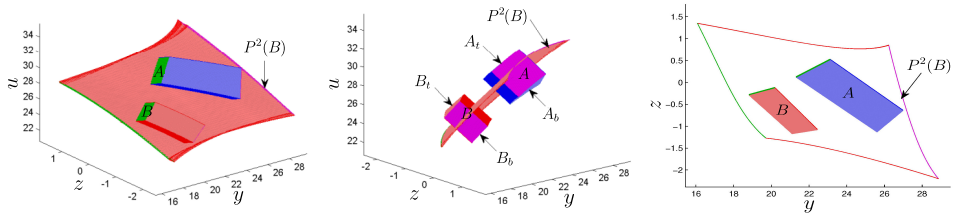

(a) 3D view (b) Side view (c) Top view

Figure 10. $P^2(B)$ separates A and B under system (1).

5 Conclusion

A new 4D hyper-chaotic system with complex dynamical behaviors is presented in this paper. The Lyapunov exponents spectrum and bifurcation diagram are provided and analyzed. The periodic orbit, chaotic, and hyper-chaotic attractors can be found in this nonlinear system. Based on the optimization method, Lyapunov stability theory, and comparison principle, we have obtained the boundedness of the new 4D hyper-chaotic system including the ultimate bound and positively invariant set Ω_1 and the globally exponentially attractive set Ω_2. The corresponding boundedness has been verified by the numerical simulations, which show the effectiveness of the proposed scheme. Besides, by means of topological horseshoe theory and numerical simulation, a topological horseshoe with two-directional expansions has been also obtained, which can rigorously ensure that system (1) is hyper-chaotic system in theory.

References

1. S.-L. Chen, S.-M. Chang, W.-W. Lin, T. Hwang, Digital secure-communication using robust hyper-chaotic systems, *Int. J. Bifurcation Chaos*, **18**(11):3325–3339, 2008.
2. L. Dieci, E.S. Van Vleck, Computation of a few Lyapunov exponents for continuous and discrete dynamical systems, *Appl. Numer. Math.*, **17**(3):275–291, 1995.
3. M.M. El-Dessoky, Synchronization and anti-synchronization of a hyperchaotic Chen system, *Chaos Solitons Fractals*, **39**(4):1790–1797, 2009.

4. M. Gidea, P. Zgliczyński, Covering relations for multidimensional dynamical systems, *J. Differ. Equations*, **202**(1):32–58, 2004.

5. X. Huang, G. Ye, An image encryption algorithm based on hyper-chaos and DNA sequence, *Multimedia Tools Appl.*, **72**(1):57–70, 2014.

6. G. Leonov, A. Bunin, N. Koksch, Attractor localization of the Lorenz system, *Z. Angew. Math. Mech.*, **67**:649–656, 1987.

7. D. Li, J.-A. Lu, X. Wu, G. Chen, Estimating the bounds for the Lorenz family of chaotic systems, *Chaos Solitons Fractals*, **23**(2):529–534, 2005.

8. D. Li, J.-A. Lu, X. Wu, G. Chen, Estimating the ultimate bound and positively invariant set for the Lorenz system and a unified chaotic system, *J. Math. Anal. Appl.*, **323**(2):844–853, 2006.

9. Q. Li, A topological horseshoe in the hyperchaotic Rossler attractor, *Phys. Lett. A*, **372**(17):2989–2994, 2008.

10. Q. Li, X. Yang, A simple method for finding topological horseshoes, *Int. J. Bifurcation Chaos*, **20**(2):467–478, 2010.

11. Q. Li, X.-S. Yang, A computer-assisted verification of hyperchaos in the saito hysteresis chaos generator, *J. Phys. A, Math. Gen.*, **39**(29):9139–9150, 2006.

12. Q. Li, X.-S. Yang, A 3D Smale horseshoe in a hyperchaotic discrete-time system, *Discrete Dyn. Nat. Soc.*, **2007**:16239, 2007.

13. Q. Li, X.-S. Yang, Hyperchaos from two coupled Wien-bridge oscillators, *Int. J. Circuit Theory Appl.*, **36**(1):19–29, 2008.

14. Q. Li, X.-S. Yang, S. Chen, Hyperchaos in a spacecraft power system, *Int. J. Circuit Theory Appl.*, **21**(6):1719–1726, 2011.

15. Q. Li, L. Zhang, F. Yang, An algorithm to automatically detect the Smale horseshoes, *Discrete Dyn. Nat. Soc.*, **2012**:283179, 2012.

16. Q.-D. Li, S. Tang, Algorithm for finding Horseshoes in three-dimensional hyperchaotic maps and its application, *Acta Phys. Sin.*, **62**(2):020510, 2013 (in Chinese).

17. X. Liao, On the global basin of attraction and positively invariant set for the Lorenz chaotic system and its application in chaos control and synchronization, *Sci. China, Ser. E*, **34**:1404–1419, 2004.

18. X. Liao, P. Yu, S. Xie, Y. Fy, Study on the global property of the smooth Chua's system, *Int. J. Bifurcation Chaos*, **16**(10):2815–2841, 2006.

19. J. Plumecoq, M. Lefranc, From template analysis to generating partitions. I: Periodic orbits, knots and symbolic encodings, *Physica D*, **144**(3–4):231–258, 2000.

20. G.Y. Qi, S. Bazebo Matondo, Hyper-chaos encryption using convolutional masking and model free unmasking, *Chin. Phys. B*, **23**(5):161–166, 2014.

21. H. Saberi Nik, S. Effati, J. Saberi-Nadjafi, New ultimate bound sets and exponential finite-time synchronization for the complex Lorenz system, *J. Complexity*, **31**(5):715–730, 2015.

22. H. Saberi Nik, S. Effati, J. Saberi-Nadjafi, Ultimate bound sets of a hyperchaotic system and its application in chaos synchronization, *J. Complexity*, **20**(4):30–44, 2015.

23. H. Saberi Nik, M. Golchaman, Chaos control of a bounded 4D chaotic system, *Neural Comput. Appl.*, **25**(3):683–692, 2014.

24. Y. Shu, W. Zhang, Y. Zhang, Boundedness and synchronization of new chaotic system, *Journal of Chongqing University of Technology*, **2010**(1):114–117, 2010.

25. A. Szymczak, The Conley index and symbolic dynamics, *Topology*, **35**(2):287–299, 1996.

26. P. Wang, D. Li, Q. Hu, Bounds of the hyper-chaotic Lorenz–Stenflo system, *Commun. Nonlinear Sci. Numer. Simul.*, **15**(9):2514–2520, 2010.

27. P. Wang, Y. Zhang, S. Tan, L. Wan, Explicit ultimate bound sets of a new hyper-chaotic system and its application in estimating the Hausdorff dimension, *Nonlinear Dyn.*, **74**(1–2):133–142, 2013.

28. Z. Wang, L. Zhou, Z. Chen, J. Wang, Local bifurcation analysis and topological horseshoe of a 4D hyper-chaotic system, *Nonlinear Dyn.*, **83**(4):2055–2066, 2016.

29. S. Wiggins, *Introduction to Applied Nonlinear Dynamical Systems and Chaos*, Texts Appl. Math., Vol. 2, Springer, New York, 1990.

30. A. Wolf, J.B. Swift, H.L. Swinney, J.A. Vastano, Determining Lyapunov exponents from a time series, *Physica D*, **16**(3):285–317, 1985.

31. X.-J. Wu, H. Wang, H.-T. Lu, Hyperchaotic secure communication via generalized function projective synchronization, *Nonlinear Anal., Real World Appl.*, **12**(2):1288–1299, 2011.

32. Z. Yan, P. Yu, Hyperchaos synchronization and control on a new hyperchaotic attractor, *Chaos Solitons Fractals*, **35**(2):333–345, 2008.

33. F. Yang, Q. Li, P. Zhou, Horseshoe in the hyperchaotic MCK circuit, *Int. J. Bifurcation Chaos*, **17**(11):4205–4211, 2007.

34. X. Yang, Topological horseshoes and computer assisted verification of chaotic dynamics, *Int. J. Circuit Theory Appl.*, **19**(4):1127–1145, 2009.

35. X. Yang, H. Li, Y. Huang, A planar topological horseshoe theory with applications to computer verifications of chaos, *J. Phys. A, Math. Gen.*, **38**(19):4175–4185, 2005.

36. P. Yu, X.X. Liao, On the study of globally exponentially attractive set of a general chaotic system, *Commun. Nonlinear Sci. Numer. Simul.*, **13**(8):1495–1507, 2008.

37. S. Zhang, T. Gao, A coding and substitution frame based on hyper-chaotic systems for secure communication, *Nonlinear Dyn.*, **84**(2):833–849, 2015.

38. T. Zhou, Y. Tang, G. Chen, Complex dynamical behaviors of the chaotic Chen's system, *Int. J. Bifurcation Chaos*, **13**(9):2561–2574, 2003.